CEPSTRAL ANALYSIS BASED BLIND DECONVOLUTION FOR MOTION BLUR

Haruka Asai, Yuji Oyamada, Julien Pilet, Hideo Saito

Graduate School of Science and Technology, Keio University
3–14–1, Hiyoshi, Kohoku, Yokohama, Japan

ABSTRACT

Camera shake during exposure blurs the captured image. Despite several decades of studies, image deconvolution to restore a blurred image still remains an issue, particularly in blind deconvolution cases in which the actual shape of the blur is unknown. Approaches based on cepstral analysis succeeded in restoring images degraded by a uniform blur caused by a camera moving straight in a single direction.

In this paper, we propose to estimate, from a single blurred image, the point spread function (PSF) caused by a normal camera undergoing a 2D curved motion, and to restore the image. To extend the traditional cepstral analysis, we derive assumptions about the PSF effects in the cepstrum domain. In a first phase, we estimate several PSF candidates from the cepstrum of a blurred image and restore the image with a fast deconvolution algorithm. In a second phase, we select the best PSF candidate by evaluating the restored images. Finally, a slower but more accurate deconvolution algorithm recovers the latent image with the chosen PSF. We validate the proposed method with synthetic and real experiments.

Index Terms— Image restoration, Blind Deconvolution, Cepstral analysis, Point spread function

1. INTRODUCTION

Researches on image deconvolution aim to recover a latent image from one or more blurred images. A blurred image g is described by a convolution of a latent image f and a point spread function (PSF) h, which represents the camera path during its exposure, plus an image noise n:

$$g = f \otimes h + n, \tag{1}$$

where $\otimes$ denotes the convolution operator. Image deconvolution deals with an inverse problem of Eq. 1. However, it is mathematically impossible to solve the inverse problem because of its ill-posedness. Thus, additional cues are required to solve the inverse problem.

Some methods try to address the blind deconvolution problem, in which the PSF is assumed as unknown. Bayesian approaches infer the most likely latent image given the observed blurred image(s) using prior knowledge about the imaging process and the nature of natural images as an additional cue [1]. However, these approaches are regarded as ad-hoc, because the result depends on learning data derived from the prior knowledge.

The other type of methods estimate PSF by analysis of the behavior of the spectrum or the cepstrum of blurred images as an additional cue. The prior works [2, 3, 4] focus on a 1D PSF. We previously aimed to extend this approach to a 2D PSF [5]. However, it lacked robustness and theoretical foundation.

In this paper, we aim to expand the target camera motion of the cepstral approach from 1D to 2D. Our main contribution is that we investigate the behavior of 1D PSF in the cepstrum domain and then derive an assumption that the PSF estimation can be done by shortest path searching in the cepstrum domain. Based on the assumption, we propose a cepstral analysis based 2D PSF estimation method. Given a single blurred image, we first estimate PSF candidates from the cepstrum of the blurred image. The candidates are evaluated from restored images computed with a fast deconvolution algorithm. Then, a slower but more precise algorithm uses the best PSF to produce the final restored image. As a result, our method achieves blind deconvolution from a single blurred image observed by a normal camera undergoing a curved 2D motion without any prior knowledge of the latent image.

2. CEPSTRAL ANALYSIS

In this section, we investigate the behavior of the cepstrum of blurred images and then derive an assumption on 2D PSF estimation in the cepstrum domain.

The cepstrum is the inverse Fourier transform of the log power spectrum of an image. When the image noise n is weak enough to neglect, the cepstrum of a blurred image C_g is approximated as the sum of the cepstrum of a PSF C_h and the cepstrum of a latent image C_f as,

$$\begin{aligned} C_g &= \mathcal{F}^{-1}\left(\log\left|\mathcal{F}\left(g\right)\right|\right) = \mathcal{F}^{-1}\left(\log\left|\mathcal{F}\left(f \otimes h + n\right)\right|\right), \\ &\approx \mathcal{F}^{-1}\left(\log\left|\mathcal{F}\left(f \otimes h\right)\right|\right), \\ &= C_f + C_h, \end{aligned} \tag{2}$$

where $\mathcal{F}$ denotes the Fourier transform.

Prior works have estimated PSF in the cepstrum domain when a PSF is a parametric form such as 1D motion param-

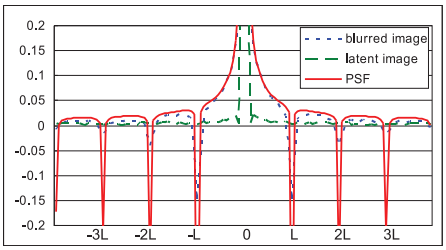

Fig. 1. Cepstrum of blurred image C_g (blue dot curve), latent image C_f (green dash curve), and PSF C_h (red curve)

eterized by the motion length L and the motion direction θ. The spectrum of 1D PSF is modeled by a sinc function, which has periodic zero values. Rom pointed that the periodic zero values are corresponding to periodic negative peaks in the cepstrum domain and the peaks appear with a period of L along with the motion direction θ [2]. Figure 1 depicts cepstra along the motion direction in the case of 1D motion blur of direction θ and length L. As [2] pointed, C_h has periodic negative peaks along with the motion direction θ and their period equals to motion length L. The shape of C_h appears hyperbolic curve with periodic negative peaks. Consider hyperbolic curve as an attenuated line proportional to distance, C_h can be regarded as a set of PSF attenuated by the distance from the positive peak and each of them appears between the adjacent peaks. Another characteristic is that C_g is dominated by C_h, especially around the positive peak. Therefore, the attenuated PSF appears most clear between the positive peak and the minimum peak, which is negative peak nearest to the positive peak.

Based on the above observation, 1D motion parameters can be estimated by finding the minimum peak. However, the latent image component C_f destabilizes finding the minimum peak. For stable detection, we use another property that C_h appears relatively stronger along the motion direction. Oliveira et al. first estimate the motion direction θ by the Radon transform and then estimate the motion length L by finding local minimum along with the estimated motion direction [3]. Ji and Liu proposed the Fourier-Radon transform to estimate the motion parameters θ and L simultaneously [4]. Therefore, we conclude that when the path integral along a path is maximum, the direction of the path denotes the direction of the motion blur.

Finally, we derive an assumption; a PSF is estimated by finding a path that maximizes the integral between the positive peak and the minimum peak in the cepstrum domain.

3. OUR APPROACH

Our method targets shift-invariant PSFs caused by a normal camera undergoing a continuous 2D curved motion. Based on the derived assumption, we proposed a method estimating 2D PSF. We start by preprocessing issues to deal with image noise. Then, we present how to estimate 2D PSF candidates, and how to select the best one.

3.1. Preprocessing

The cepstrum of a blurred image C_g has a property that the PSF component C_h dominates the cepstrum around the positive peak. To use C_h for PSF estimation, the latent image component C_f and also image noise n is an obstacle component. To reduce the contribution of C_f and also n, we utilize the shift-variability of natural images and image noise. A shift-invariant PSF remains constant over the whole image while natural images and image noise are shift-variant. The contribution of the sub-images of shift-variant components whereas the one of PSF is constant. Thus, the contribution of shift-variant components is reduced by taking an average of all cepstrum of sub-images. We first partition a blurred image into sub-images and then take average of all the cepstra of sub-images.

In the cepstrum domain, the minimum peak plays an important role for cepstral analysis but it is sometimes too weak to be detected reliably due to the image noise. Instead of finding the minimum peak, we extract several local minima $l_i (i = 1, \cdots, N)$ as candidates from the average cepstrum $\overline{C_g}$. We consider that the minimum peak is included in these several local minima.

3.2. PSF candidates estimation

Now, we have the average cepstrum of the blurred image $\overline{C_g}$ and N extracted local minima. Based on the derived assumption, we estimate a PSF by finding a path maximizing integral between the positive peak and a local minimum in the cepstrum domain. Because we assume constant speed camera motion, PSF shape estimation is sufficient. Thus, this problem can be regarded as a kind of path searching problem. We apply dynamic programming to solve this problem.

Consider that we take integral from a local minimum (P, Q) to the positive peak $(0, 0)$. Distance from the local minimum (P, Q) to a current position (p, q) is calculated as

$$\begin{aligned} \mathrm{dist}(p,q) &= \max\left(d_{p,q} + \mathrm{cost}(p+\Delta p, q+\Delta q)\overline{C_g}(p,q)\right), \quad (3) \\ d_{p,q} &= \mathrm{dist}(p+\Delta p, q+\Delta q), \end{aligned}$$

where $(\Delta p, \Delta q) \in (0,1), (1,1), (1,0)$. For each cost value $\mathrm{cost}(p+\Delta p, q+\Delta q)$, we consider the connectivity between (p, q) and $(0, 0)$. The estimated path should favour smooth curve or straight line not zigzag line because it represents camera path. Thus, we set the cost function as follows,

$$\mathrm{cost}\,(p+\Delta p, q+\Delta q) = \frac{\langle \overrightarrow{v}_{P,Q}, \overrightarrow{v}_{p+\Delta p,q+\Delta q} \rangle}{\|\overrightarrow{v}_{P,Q}\| \cdot \|\overrightarrow{v}_{p+\Delta p,q+\Delta q}\|},$$

$$\overrightarrow{v}_{j,k} = \overrightarrow{(j,k)},$$

where $\overrightarrow{v}_{j,k}$ denotes the vector from current position (j,k) to (P,Q). After taking integral from the local minimum to the positive peak, we find a path maximizing integral as a shape of PSF. Because we assume constant speed camera motion, we assign uniform intensity to the PSF. Totally, N PSF candidates $\hat{h}_i$ are extracted and each of them are corresponding to each local minimum l_i.

3.3. PSF candidates evaluation

Now, we have N PSF candidates $\hat{h}_i$, each of which has different shape. Since it is difficult to evaluate PSF candidate itself, we use the restored image instead of PSF candidate for evaluation.

Most likely PSF is computed as

$$\hat{h} = \arg\min_{\hat{h}_i} \left(\left| g - \hat{f}_i \otimes \hat{h}_i \right| + \lambda \sqrt{P_i^2 + Q_i^2} \right), \quad (4)$$

where $\hat{f}_i$ denotes the restored image recovered by $\hat{h}_i$, (P_i, Q_i) denotes the position of i th local minimum. The first term evaluates ringing artifacts. When we restore a blurred image with a wrong PSF, the restored image has ringing artifacts. Since the latent image is unknown, we blur the restored image and compare it with the blurred image. The first term has a minimum when the PSF candidate is correct in theory but has another minimum when the PSF is a delta function, corresponding to the identity transformation. To avoid favoring delta function, we add the second term as a regularization term.

Because the cepstrum is symmetrical about the positive peak, a set of $\hat{h}_i$ has redundancy about symmetry. Thus, we first eliminate the ambiguity about the shape and then the ambiguity about symmetry. For shape ambiguity, we choose Wiener filtering [6] as a deconvolution algorithm because of two reasons. First, because it works in the frequency domain, the symmetry does not affect the restored image. Second, its computational requirement is reasonable. In this manner, we choose a PSF $\hat{h}$ from N candidates by evaluating Eq. 4. Next, we make a symmetric PSF $\hat{h}_{\text{sym}}$from $\hat{h}$. We restore the blurred image by Richardson-Lucy algorithm [7, 8] and evaluate these two PSFs based on Eq. 4. Finally, we obtain the most likely PSF $\hat{h}$.

4. EXPERIMENTAL RESULT

We performed two experiments using synthetic images and real images to validate the proposed method. Through the experiments, we apply a deconvolution method [9] proposed by Levin et al.

Synthetic experiments. In the synthetic experiment, we use 100 images of 321×241 resolution, randomly chosen from The Berkeley Segmentation Dataset, and 5 PSFs leading 500 blurred images. Figure 2 shows the enlarged PSFs which original size are written in captions. Note that the width of all the PSFs is 1 pixel. For each image, we computed the Peak Signal-to-Noise Ratio (PSNR) of the blurred image PSNR(g) and the one of the restored image PSNR$(\hat{f})$ and then computed the PSNR ratio PSNR$(\hat{f})$/PSNR(g). The ratio greater than 1.0 means that the restored image is closer to the original image than the blurred image. Table 1 shows the number of cases of which ratio is greater than 1.0 with respect to each PSF. Top row shows the result using raw cepstrum, skipping the preprocessing, and bottom row shows the result of the proposed method. Except PSF1, more than 90 of 100 blurred images result in the ratio greater than 1.0. The reason why PSF1 results in relatively worse than others is because of its energy. When a PSF has smaller size, the cepstrum of the PSF has also smaller energy. In such case (e.g., PSF1 of w/o case), C_h does not dominate C_g, then the proposed method fails. On the other hand, w/ cases including our preprocessing provided better result. This result indicates that the performance of the preprocessing can reduce the contribution of the latent image component C_f. Next, we added i.i.d. Gaussian noises with varying variances to blurred images and then applied our method to examine the effect of image noise. Table 2 shows the result of 500 trials. From top to bottom, the average value of PSNR(g), the average value of PSNR$(\hat{f})$ and the number of success of 500 trials are shown. A successful case means a case which PSNR ratio is greater than 1.0. Comparison of the average value of PSNR(g) and one of PSNR$(\hat{f})$ shows that the restored images are closer to the original images than the blurred images. The result of the number of success indicates that our method results in better result more than 80 percent even with image noise.

Fig. 2. 5 PSFs for synthetic experiments with their size.

Table 1. Deconvolution result of synthetic images.

	PSF1	PSF2	PSF3	PSF4	PSF5
w/o	34	96	91	100	91
w/	71	96	98	100	98

Table 2. Deconvolution result under varying image noise.

Variance	0	5	10	15	20
PSNR(g)	22.6	22.5	22.3	22.2	22.1
PSNR$(\hat{f})$	24.2	24.2	24.0	23.8	23.5
# success	463	459	455	444	434

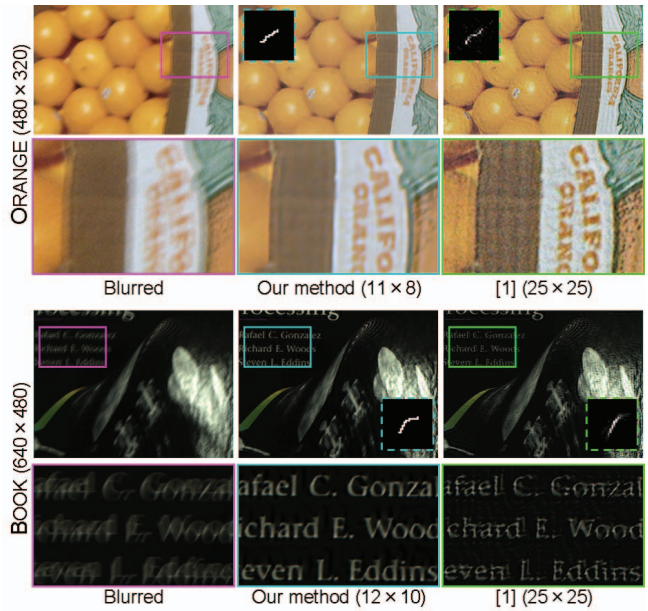

Fig. 3. Deconvolution result of real images. From left to right, blurred image, restored image by our method, restored image by [1] are shown.

Real world experiments. In the real world experiment, we compare the proposed method with a Bayesian approach [1] to validate the proposed method. Figure 3 shows the result of two scenes with their resolution. Each caption of our method and [1] denotes the size of estimated PSF. Dashed frame in the figure shows estimated PSF. Second and fourth rows are zoom-up of framed region in first and third rows respectively. On the ORANGE scene, both the restored images by our method and [1] get clearer and sharper, especially text on the image is more readable on the restored images. This result indicates that both methods estimate PSF closer to the correct one. On the other hand, [1] recovers the latent image including artifact on the BOOK scene while our method gets clearer restored image. One of the reasons [1] failed is their assumption. Bayesian approaches utilize the natural image statistics for PSF estimation. The book scene consists of text, bright region on the right side, and few pictures on the left side. The property of such scene is difficult to describe by the natural image statistics. Other results will be available on the project webpage (`http://www.hvrl.ics.keio.ac.jp/~charmie/work/id/icip2010/`).

5. CONCLUSION

In this paper, we focus on blind deconvolution for a single blurred image taken by a normal camera undergoing a curved 2D motion. We identified the characteristics of the cepstrum of PSFs and derived the assumption. Basic idea of the our method is that the PSF is estimated by finding a path which maximizes integral between the positive peak and the minimum peak in the cepstrum domain. Our method relies on dynamic programming to find these paths, yielding PSF candidates. The candidates are evaluated from restored images computed with a fast deconvolution algorithm. A slower but more precise algorithm then uses the best PSF to produce the final restored image. The our method is applied for both synthetic images and real images for validation. As experimental results show, our method achieves blind deconvolution from a single blurred image observed by a normal camera undergoing a curved 2D motion.

Acknowledgement

This work is supported in part by a Grant-in-Aid for the GCOE for high-Level Global Cooperation for Leading-Edge Platform on Access Spaces from MEXT, Japan.

6. REFERENCES

[1] Rob Fergus, Barun Singh, Aaron Hertzmann, Sam T. Roweis, and William T. Freeman, "Removing camera shake from a single photograph," *ACM Transactions on Graphics*, vol. 25, no. 3, pp. 787–794, 2006.

[2] Raphael Rom, "On the cepstrum of two-dimensional functions," *IEEE Transactions on Information Theory*, vol. 21, no. 2, pp. 214–217, 1975.

[3] Joao P. Oliveira, Mario A.T. Figueiredo, and Jose M. Bioucas-Dias, "Blind estimation of motion blur parameters for image deconvolution," in *3rd Iberian conference on Pattern Recognition and Image Analysis, Part II (IbPRIA)*, 2007.

[4] Hui Ji and Chaoqiang Liu, "Motion blur identification from image gradients," in *IEEE Conference on Computer Vision and Pattern Recognition (CVPR)*, 2008.

[5] Yuji Oyamada, Hideo Saito, Koji Ootagaki, and Mitsuo Eguchi, "Cepstrum based blind image deconvolution," in *International Workshop on Vision, Communications and Circuits*, 2008, pp. 197–201.

[6] Wiener Norbert, "Extrapolation, interpolation, and smoothing of stationary time series," 1949.

[7] William Hadley Richardson, "Bayesian-based iterative method of image restoration," *Journal of the Optical Society of America*, vol. 62, no. 1, pp. 55–59, 1972.

[8] L. B. Lucy, "An iterative technique for the rectification of observed distributions," *The Astronomical Journal*, vol. 79, pp. 745–754, 1974.

[9] Anat Levin, Rob Fergus, Fredo Durand, and William T. Freeman, "Image and depth from a conventional camera with a coded aperture," *ACM Transactions on Graphics*, vol. 26, pp. 1–10, 2007.